18th International Conference on Information Fusion
Washington, DC - July 6-9, 2015

Bearings-Only Tracking with Fusion from Heterogenous Passive Sensors: ESM/EO and Acoustic

Rong Yang, Gee Wah Ng
DSO National Laboratories,
20 Science Park Drive, Singapore 118230
Emails: {yrong,ngeewah}@dso.org.sg

Yaakov Bar-Shalom
Department of ECE,
University of Connecticut,
Storrs, CT 06269, USA
Email: ybs@engr.uconn.edu

***Abstract*—The performance of the conventional bearings-only tracking (BOT) from a single passive sensor largely depends on the sensor platform maneuvers. This paper presents a new BOT approach based on fusion from two heterogenous bearings-only sensors residing on the same moving or stationary platform. The two sensors are an ESM/EO with negligible propagation delay and an acoustic sensor with significant propagation delay. Since target range information is contained in the acoustic propagation delay, the problem is therefore observable even when the platform is stationary. An out-of-sequence measurement fusion from the acoustic and ESM/EO sensors (OOSM-AE) is developed to estimate the target trajectory. It consists of an unscented Kalman filter (UKF) to handle in-sequence ESM/EO measurements and an OOSM unscented Gauss-Helmert filter (OOSM-UGHF) to handle out-of-sequence acoustic measurements. Simulation tests are conducted to demonstrate the performance of this new BOT approach.**

***Keywords*—Propagation delay, bearings-only tracking, target motion analysis, unscented Gauss-Helmert filter, out-of-sequence measurement.**

I. Introduction

The commonly used passive sensors, like acoustic sensors, electronic support measures (ESM) sensors and electro-optical (EO) sensors, detect target bearings only. This makes the target trajectory estimation from range-absent measurements a challenging problem.

Several approaches have been developed in the last four decades. The most popular one is to deploy a passive sensor on a maneuvering platform, and the target trajectory is estimated using bearings-only tracking (BOT) or bearings-only target motion analysis (BO-TMA) [15] [1]. This approach requires the sensor platform to maneuver, so the target trajectory is observable [16] [11] [6]. Since these maneuvers can interfere with the sensor platform's own mission (for example: to reach its destination as early as possible), BOT from a nonmaneuvering sensor has attracted attention recently. Results showed that the BOT problem is indeed observable from a nonmaneuvering sensor when a target is performing particular maneuvers (two-leg with constant speed, or constant turn) [12] [7]. However, there is still a gap to transition these results to real applications, for the target can maneuver in a manner unbeknownst to the observer, and the nearly constant velocity (CV) motion is the common motion used in operation.

The BOT approach has been extended to the Doppler-bearing tracking (DBT) approach in [17] [10]. This approach tracks target position and emitted frequencies from bearings and Doppler shifted frequencies and a target trajectory can be estimated even when the platform is not maneuvering. The difficulty faced in DBT is to identify target frequencies from a noisy environment, especially when the target emitted frequencies are varying.

Another approach is to locate targets through triangulation from multiple stationary or moving passive sensors located at different positions. This approach needs to remove triangulation "ghosts" in multi-target scenarios, and can be solved as an S-D assignment problem, where S is the number of sensors. A Lagrangian relaxation was suggested to solve the problem when $S \geq 3$ [18] [8]. By making use of Doppler frequencies, the number of sensors can be reduced to 2 ($S = 2$) [20].

In this paper, we propose a new bearings-only approach to fuse measurements from two heterogenous passive sensors deployed on the same platform which can be *either moving or stationary*. The two sensors are a passive ESM/EO sensor, designated as s_1 and a passive acoustic sensor, designated as s_2. Both sensors detect target bearings only. The ESM/EO sensor's detections have no propagation delay, whereas the acoustic sensor receives the target signals after significant propagation delays. The time difference between the reception times of the two sensors is the acoustic propagation delay, and the target range can then be inferred from the estimates of these delays assuming the propagation speed is known. Complete observability in this BOT problem is therefore obtained, as range is implied in the sensors' reception times.

However, to obtain target range using the principle mentioned above is not straightforward. To compute the acoustic propagation delay, a pair of passive signals from s_1 and s_2 having the same emission time needs to be identified. A BOT target usually emits continuous signals which are received by the sensors and discretized by sampling. They are not instantaneous signals, like "ping" or "pulse" which can be associated easily. There is no feature to identify an acoustic

Yaakov Bar-Shalom was supported by ARO Grant W991NF-10-1-0369.
Proc. 18th Intn'l Conf. on Information Fusion, Washington, D.C., USA, July 2015.

bearing measurement and an ESM/EO measurement emitted at the same time. Furthermore, the ESM/EO and acoustic sensor may have different sampling times (they are asynchronous), and the sensor platform may be dynamic. These make the problem even more complicated. A comprehensive algorithm is therefore needed to take all these issues into consideration.

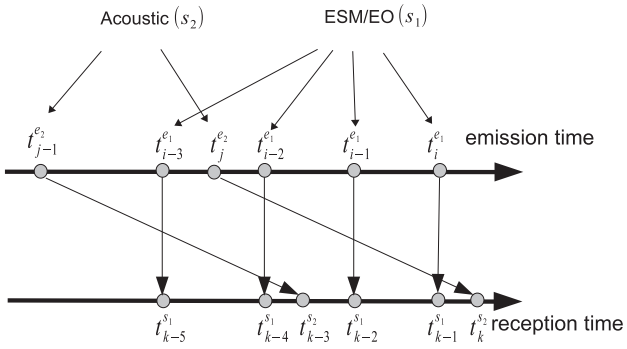

Fig. 1. Out-of-sequence measurements in ESM/EO and acoustic sensors.

Fig. 1 illustrates the ESM/EO and acoustic signal emission and reception time sequences, where k is the reception time index, which orders the combined acoustic and EO/ESM discretized signals by arrival (sensor) time. This is also the measurement index, while i and j are the target signal emission time indexes from s_1 and s_2, respectively. It can be seen that out-of-sequence measurements (OOSM) occur due to the acoustic propagation delay.

The OOSM problem is also referred to as "negative-time measurement update" problem, namely, the state time, $t_j^{e_2}$, corresponding to the latest measurement at $t_k^{s_2}$ is earlier than the latest state updating time, $t_i^{e_1}$, namely $t_j^{e_2} < t_i^{e_1}$ The prediction step in the in-sequence estimation becomes a retrodiction in the OOSM. The OOSM problem has been well studied [5]. The simplest approach performs an approximate retrodiction by neglecting the process noise [5]. This approach is referred to as Algorithm C [5]. Algorithms B1 and A1 were proposed to solve the one-step-lag OOSM by considering process noise [9] [3], and they give an approximate and the exact solutions, respectively. They were further developed to the algorithms Bl1 and Al1 for solving the l-step-lag OOSM ($l > 1$) in a single step [4].

The existing OOSM algorithms mentioned above assume that retrodiction time is known. However, the retrodiction time is the acoustic signal emission time in our problem. This is unknown to the observer and depends on the state of the target which is given by the following propagation delay constraint:

$$t_j^{e_2} = t_k^{s_2} - \delta_j \tag{1}$$

where

$$\delta_j = \frac{r_j}{c^{\mathrm{p}}} \tag{2}$$

is the propagation delay, c^{p} is the signal propagation speed in the medium, and r_j, which depends on the state (at the emission time), is the distance from the target at time $t_j^{e_2}$ to the sensor at time $t_k^{s_2}$. This leads to an implicit constraint in state transition model.

Recently, we have formulated implicit constraint dynamic estimation problem to a Gauss-Helmert model (GHM), and proposed an unscented Gauss-Helmert filter (UGHF) [22] [21] to solve this problem. The existing UGHF works with in-sequence measurements. Further development on OOSM-UGHF is presented in this paper.

The aim of this paper is to develop a comprehensive algorithm to estimate states with fusion of in-sequence bearings from the ESM/EO sensor (s_1) and out-of-sequence bearings from the acoustic sensor (s_2). State estimation for the bearings from s_1 will be performed by a unscented Kalman filter (UKF), and for s_2, a new OOSM-UGHF will be developed. They are described in the following sections.

Unscented transform (UT) is selected to approximate nonlinear transformations in both in-sequence and out-of-sequence estimations in this paper. This is because it provides better accuracy than the first-order Taylor linearization (used in the extended Kalman filter) by accounting for the asymmetry of the nonlinear transformation. Compared to the particle filtering approach, a UT is orders of magnitude less demanding computationally. The UT has advantages in both estimation accuracy and efficiency, which are important factors in real applications.

II. State Estimation with the ESM/EO Sensor

The state estimation for the ESM/EO bearings is straightforward as the measurement is in-sequence and no propagation delay needs to be taken into consideration. The problem is formulated based on the nearly CV state model (or WNA — white noise acceleration). The target state with size 4 is defined as

$$\mathbf{x}^4(t_k^{s_1}) = \begin{bmatrix} x(t_k^{s_1}) & y(t_k^{s_1}) & \dot{x}(t_k^{s_1}) & \dot{y}(t_k^{s_1}) \end{bmatrix}' \tag{3}$$

where $t_k^{s_1}$ is the signal reception (or sensor) time by the ESM/EO sensor s_1 at time cycle k. Since the propagation delay is negligible for s_1, the target signal emission time $t_i^{e_1}$ is equal to $t_k^{s_1}$. The state transition model is[1]

$$\mathbf{x}^4(t_k^{s_1}) = \mathbf{F}(t_k^{s_1}, t_{k-1}^{s_1})\mathbf{x}^4(t_{k-1}^{s_1}) + \mathbf{v}^4(t_k^{s_1}, t_{k-1}^{s_1}) \tag{4}$$

where the transition matrix is

$$\mathbf{F}(t_k^{s_1}, t_{k-1}^{s_1}) = \begin{bmatrix} 1 & 0 & T_{k,k-1} & 0 \\ 0 & 1 & 0 & T_{k,k-1} \\ 0 & 0 & 1 & 0 \\ 0 & 0 & 0 & 1 \end{bmatrix} \tag{5}$$

and

$$T_{k,k-1} = t_k^{s_1} - t_{k-1}^{s_1} \tag{6}$$

with $\mathbf{v}^4$ the zero-mean process noise (WNA) for the interval $(t_k^{s_1}, t_{k-1}^{s_1}]$. The resulting discretized white noise acceleration (DWNA) model [2] has covariance

$$\mathbf{Q}^4(t_k^{s_1}, t_{k-1}^{s_1}) = \begin{bmatrix} \frac{T_{k,k-1}^3}{3} & 0 & \frac{T_{k,k-1}^2}{2} & 0 \\ 0 & \frac{T_{k,k-1}^3}{3} & 0 & \frac{T_{k,k-1}^2}{2} \\ \frac{T_{k,k-1}^2}{2} & 0 & T_{k,k-1} & 0 \\ 0 & \frac{T_{k,k-1}^2}{2} & 0 & T_{k,k-1} \end{bmatrix} q \tag{7}$$

[1]Here it is assumed for simplicity that the measurements arriving at t_{k-1} and t_k are both from sensor s_1.

where q is power spectral density (PSD) of the motion process noise (same for x and y, and assumed independent between the coordinates). The measurement model is given by

$$z(t_k^{s_1}) = b(t_k^{s_1}) = \tan^{-1}\left[\frac{x(t_k^{s_1}) - x^s(t_k^{s_1})}{y(t_k^{s_1}) - y^s(t_k^{s_1})}\right] + w(t_k^{s_1}) \quad (8)$$

where $x^s(t_k^{s_1})$ and $y^s(t_k^{s_1})$ are the sensor positions at time $t_k^{s_1}$ in the x and y coordinates respectively, $w(t_k^{s_1})$ is zero-mean white Gaussian measurement noise with variance $R(t_k^{s_1})$, assumed independent of the process noise.

The unscented Kalman filter (UKF) is used to estimate the state [13].

III. State Estimation with the Acoustic Sensor

An out-of-sequence-measurement filter is required for the bearings from the acoustic sensor s_2. It can be seen in Fig. 1 that an acoustic measurement received at time $t_k^{s_2}$ corresponds to the target state at emission time $t_j^{e_2}$, which is earlier than the latest state assumed to have been updated by the ESM/EO sensor at time $t_{k-1}^{s_1} = t_i^{e_1}$. The problem is then to update the state estimate $\hat{\mathbf{x}}^4(t_{k-1}^{s_1}|t_{k-1}^{s_1})$ with the acoustic measurement $z(t_k^{s_2})$. The main challenge of this problem compared to the existing OOSM approaches is that the time $t_j^{e_2}$ is unknown, and it needs to be estimated together with the kinematic state.

The OOSM approach to address the above mentioned problem consists of the following steps:

- Retrodict the state from time $t_i^{e_1} = t_{k-1}^{s_1}$ to the (unknown) emission time $t_j^{e_2}$ (to be estimated) corresponding to the sensor time $t_k^{s_2}$. The state before retrodiction is $\hat{\mathbf{x}}^4(t_{k-1}^{s_1}|t_{k-1}^{s_1})$, and the state after retrodiction is $\hat{\mathbf{x}}^5(t_j^{e_2}|t_{k-1}^{s_1})$. The latter, defined in (9), includes the acoustic emission time.
- Update the state estimate $\hat{\mathbf{x}}^4(t_{k-1}^{s_1}|t_{k-1}^{s_1})$ to $\hat{\mathbf{x}}^4(t_{k-1}^{s_1}|t_k^{s_2})$ by the acoustic OOSM $z(t_k^{s_2})$.

The unscented transform is used in the above two steps instead of the first-order Taylor linearization used in the existing OOSM algorithms [4] [5].

A. State Retrodiction

The retrodiction has to be done to the emission time $t_j^{e_2}$ that is unknown to the observer, but can be derived from the propagation delay constraint described in (1). To estimate the retrodicted target kinematic information and the emission time $t_j^{e_2}$ simultaneously, the following augmented state is defined:

$$\mathbf{x}^5(t_j^{e_2}) = \begin{bmatrix} x(t_j^{e_2}) & y(t_j^{e_2}) & \dot{x}(t_j^{e_2}) & \dot{y}(t_j^{e_2}) & t_j^{e_2} \end{bmatrix}' \quad (9)$$

Obviously, the positions $x(t_j^{e_2})$, $y(t_j^{e_2})$ and the time $t_j^{e_2}$ depend on each other, and this leads to the retrodicted state $\hat{\mathbf{x}}^5(t_j^{e_2}|t_{k-1}^{s_1})$ and the latest state estimate $\hat{\mathbf{x}}^4(t_{k-1}^{s_1}|t_{k-1}^{s_1})$ to have an implicit relationship. The Gauss-Helmert transition model [22] [21], which handles such implicit relationships, is then used for retrodiction. This is described by

$$\mathbf{g}\left[\mathbf{x}^5(t_j^{e_2}), \mathbf{x}^4(t_{k-1}^{s_1})\right] + \mathbf{v}^5(t_{k-1}^{s_1}, t_j^{e_2}) = \mathbf{0}_5 \quad (10)$$

where $\mathbf{g}[\cdot]$ is the Gauss-Helmert implicit state transition function, which combines the target motion constraints and the delay constraint between $\mathbf{x}^5(t_j^{e_2})$ of dimension 5 and $\mathbf{x}^4(t_{k-1}^{s_1})$ of dimension 4. Assuming the target motion follows a WNA motion, $\mathbf{g}[\cdot]$ is given by

$$\mathbf{g}[\cdot] = \begin{bmatrix} g_1(\cdot) & g_2(\cdot) & g_3(\cdot) & g_4(\cdot) & g_5(\cdot) \end{bmatrix}' \quad (11)$$

where

$$\begin{aligned} g_1 &= x(t_j^{e_2}) - x(t_{k-1}^{s_1}) - \dot{x}(t_{k-1}^{s_1})T_{j,k-1} && (12)\\ g_2 &= y(t_j^{e_2}) - y(t_{k-1}^{s_1}) - \dot{y}(t_{k-1}^{s_1})T_{j,k-1} && (13)\\ g_3 &= \dot{x}(t_j^{e_2}) - \dot{x}(t_{k-1}^{s_1}) && (14)\\ g_4 &= \dot{y}(t_j^{e_2}) - \dot{y}(t_{k-1}^{s_1}) && (15)\\ g_5 &= t_j^{e_2} + \frac{r_j}{c^{\mathrm{p}}} - t_k^{s_2} && (16) \end{aligned}$$

and

$$T_{j,k-1} = t_j^{e_2} - t_{k-1}^{s_1} < 0 \quad (17)$$

$$r_j = \sqrt{[x(t_j^{e_2}) - x^s(t_k^{s_2})]^2 + [y(t_j^{e_2}) - y^s(t_k^{s_2})]^2} \quad (18)$$

Note that Eq. (16) is the one that connects the emission time and location to the corresponding sensor reception time.

The process noise $\mathbf{v}^5$ is the zero-mean Gaussian. Based on the DWNA model [5], its covariance is

$$\mathbf{Q}^5(t_j^{e_2}, t_{k-1}^{s_1}) = \begin{bmatrix} \frac{|T_{j,k-1}|^3}{3}q & 0 & \frac{T_{j,k-1}^2}{2}q & 0 & 0 \\ 0 & \frac{|T_{j,k-1}|^3}{3}q & 0 & \frac{T_{j,k-1}^2}{2}q & 0 \\ \frac{T_{j,k-1}^2}{2}q & 0 & |T_{j,k-1}|q & 0 & 0 \\ 0 & \frac{T_{j,k-1}^2}{2}q & 0 & |T_{j,k-1}|q & 0 \\ 0 & 0 & 0 & 0 & q_\delta \end{bmatrix} \quad (19)$$

where q is as in (7), and q_δ is the variance of the process noise in the delay.

The algorithm used for retrodiction is the UGHF [22] [21], which obtains the retrodicted state iteratively through a Gauss-Newton algorithm. Given $\hat{\mathbf{x}}^4(t_{k-1}^{s_1}|t_{k-1}^{s_1})$ and its error covariance $\mathbf{P}^4(t_{k-1}^{s_1}|t_{k-1}^{s_1})$, the sigma points and their corresponding weights are

$$\begin{aligned} &\left[\{\hat{\mathbf{x}}^{4,m}(t_{k-1}^{s_1}|t_{k-1}^{s_1})\}, \{w^m\}\right] = \\ &\quad \text{SigmaPts}\left[\hat{\mathbf{x}}^4(t_{k-1}^{s_1}|t_{k-1}^{s_1}), \mathbf{P}^4(t_{k-1}^{s_1}|t_{k-1}^{s_1}), \kappa\right] && (20) \end{aligned}$$

where

$$\begin{aligned} \hat{\mathbf{x}}^{4,0}(t_{k-1}^{s_1}|t_{k-1}^{s_1}) &= \hat{\mathbf{x}}^4(t_{k-1}^{s_1}|t_{k-1}^{s_1}) && (21)\\ \hat{\mathbf{x}}^{4,m}(t_{k-1}^{s_1}|t_{k-1}^{s_1}) &= \hat{\mathbf{x}}^4(t_{k-1}^{s_1}|t_{k-1}^{s_1}) && (22)\\ &\quad + \left[\sqrt{(4+\kappa)\mathbf{P}^4(t_{k-1}^{s_1}|t_{k-1}^{s_1})}\right]_{|m|} \\ &\quad (\mathrm{m} = 1, \ldots, 4) \\ \hat{\mathbf{x}}^{4,m}(t_{k-1}^{s_1}|t_{k-1}^{s_1}) &= \hat{\mathbf{x}}^4(t_{k-1}^{s_1}|t_{k-1}^{s_1}) && (23)\\ &\quad - \left[\sqrt{(4+\kappa)\mathbf{P}^4(t_{k-1}^{s_1}|t_{k-1}^{s_1})}\right]_{|m|} \\ &\quad (\mathrm{m} = -4, \ldots, -1) \end{aligned}$$

$$\begin{aligned} w^0 &= \frac{\kappa}{4+\kappa} && (24)\\ w^m &= \frac{1}{2(4+\kappa)} \qquad |m| = 1, \cdots, 4 && (25) \end{aligned}$$

where $m = -4, \ldots, 4$, is the sigma point index, $\left[\sqrt{(4+\kappa)\mathbf{P}(t^e_{k-1}|t^{s_1}_{k-1})}\,\right]_{|m|}$ indicates the $|m|$th column of the matrix $\left[\sqrt{(4+\kappa)\mathbf{P}^4(t^{s_1}_{k-1}|t^{s_1}_{k-1})}\,\right]$, and κ is a scalar that determines the spread of sigma points. Each sigma point is retrodicted from the previous target time $t^{s_1}_{k-1}$ to an unknown time $(t^{e_2}_j)^m$. The problem is then to solve

$$\mathbf{g}\left[\hat{\mathbf{x}}^{5,m}(t^{e_2}_j|t^{s_1}_{k-1}), \hat{\mathbf{x}}^{4,m}(t^{s_1}_{k-1}|t^{s_1}_{k-1})\right] = \mathbf{0}_5 \quad m = -4, \ldots, 4 \tag{26}$$

Note that the process noise is not taken into consideration in the OOSM algorithm C.

A Gauss-Newton algorithm is applied to obtain the points $\hat{\mathbf{x}}^{5,m}(t^{e_2}_j|t^{s_1}_{k-1})$ iteratively. The iteration procedure (with index n) for the mth sigma point is

$$\begin{aligned}[\hat{\mathbf{x}}^{5,m}(t^{e_2}_j|t^{s_1}_{k-1})]^n &= [\hat{\mathbf{x}}^{5,m}(t^{e_2}_j|t^{s_1}_{k-1})]^{n-1} + \mathbf{A}^{-1} \\ &\times \mathbf{g}\left[[\hat{\mathbf{x}}^{5,m}(t^{e_2}_j|t^{s_1}_{k-1})]^{n-1}, \hat{\mathbf{x}}^{4,m}(t^{s_1}_{k-1}|t^{s_1}_{k-1})\right]\end{aligned} \tag{27}$$

where $\mathbf{A}$ (without arguments, for conciseness) is the Jacobian matrix given by

$$\begin{aligned}\mathbf{A} &= \frac{\partial \mathbf{g}\left[\left[\hat{\mathbf{x}}^{5,m}(t^{e_2}_j|t^{s_1}_{k-1})\right]^n, \hat{\mathbf{x}}^{4,m}(t^{s_1}_{k-1}|t^{s_1}_{k-1})\right]}{\partial\left[\hat{\mathbf{x}}^{5,m}(t^{e_2}_j|t^{s_1}_{k-1})\right]^n} \\ &= \begin{bmatrix} 1 & 0 & 0 & 0 & -\dot{x}^m(t^{s_1}_{k-1}|t^{s_1}_{k-1}) \\ 0 & 1 & 0 & 0 & -\dot{y}^m(t^{s_1}_{k-1}|t^{s_1}_{k-1}) \\ 0 & 0 & 1 & 0 & 0 \\ 0 & 0 & 0 & 1 & 0 \\ \dfrac{x^r_j}{r_j c^{\mathrm{p}}} & \dfrac{y^r_j}{r_j c^{\mathrm{p}}} & 0 & 0 & 1 \end{bmatrix}\end{aligned} \tag{28}$$

and

$$x^r_j \triangleq [x^m(t^{e_2}_j|t^{s_1}_{k-1})]^n - x^s(t^{s_2}_k) \tag{29}$$

$$y^r_j \triangleq [y^m(t^{e_2}_j|t^{s_1}_{k-1})]^n - y^s(t^{s_2}_k) \tag{30}$$

$$r_j \triangleq \sqrt{(x^r_j)^2 + (y^r_j)^2} \tag{31}$$

The initial of the mth sigma point $[\hat{\mathbf{x}}^{5,m}(t^{e_2}_j|t^{s_1}_{k-1})]^0$ for the iteration process in (27) is computed approximately by

$$[x^m(t^{e_2}_j|t^{s_1}_{k-1})]^0 = x^m(t^{s_1}_{k-1}|t^{s_1}_{k-1}) + \dot{x}^m(t^{s_1}_{k-1}|t^{s_1}_{k-1}) \times [\Delta(t^{e_2}_j)]^0 \tag{32}$$

$$[y^m(t^{e_2}_j|t^{s_1}_{k-1})]^0 = y^m(t^{s_1}_{k-1}|t^{s_1}_{k-1}) + \dot{y}^m(t^{s_1}_{k-1}|t^{s_1}_{k-1}) \times [\Delta(t^{e_2}_j)]^0 \tag{33}$$

$$[\dot{x}^m(t^{e_2}_j|t^{s_1}_{k-1})]^0 = \dot{x}^m(t^{s_1}_{k-1}|t^{s_1}_{k-1}) \tag{34}$$

$$[\dot{y}^m(t^{e_2}_j|t^{s_1}_{k-1})]^0 = \dot{y}^m(t^{s_1}_{k-1}|t^{s_1}_{k-1}) \tag{35}$$

$$[(t^{e_2}_j)^m]^0 = t^{s_2}_k - \delta_j \tag{36}$$

where

$$[\Delta(t^{e_2}_j)]^0 = [(t^{e_2}_j)^m]^0 - t^{s_1}_{k-1} \tag{37}$$

$$\delta_j \approx r^m_{k-1}/c^{\mathrm{p}} \tag{38}$$

and r^m_{k-1} is the distance between the target estimate and the sensor at time $t^{s_1}_{k-1}$.

The retrodicted state $\hat{\mathbf{x}}^5(t^{e_2}_j|t^{s_1}_{k-1})$ and its error covariance $\mathbf{P}^5(t^{e_2}_j|t^{s_1}_{k-1})$ are then computed from weighted sums of the retrodicted sigma points.

$$\hat{\mathbf{x}}^5(t^{e_2}_j|t^{s_1}_{k-1}) = \sum_{m=-4}^{4} w^m \hat{\mathbf{x}}^{5,m}(t^{e_2}_j|t^{s_1}_{k-1}) \tag{39}$$

$$\mathbf{P}^5(t^{e_2}_j|t^{s_1}_{k-1}) \approx \sum_{m=-4}^{4} w^m \tilde{\mathbf{x}}^{5,m}(t^{e_2}_j|t^{s_1}_{k-1})(\tilde{\mathbf{x}}^{5,m}(t^{e_2}_j|t^{s_1}_{k-1}))' \tag{40}$$

where

$$\tilde{\mathbf{x}}^{5,m}(t^{e_2}_j|t^{s_1}_{k-1}) = \hat{\mathbf{x}}^{5,m}(t^{e_2}_j|t^{s_1}_{k-1}) - \hat{\mathbf{x}}^5(t^{e_2}_j|t^{s_1}_{k-1}) \tag{41}$$

with $m = -4, \ldots, 4$.

B. State Update

This step updates $\hat{\mathbf{x}}^4(t^{s_1}_{k-1}|t^{s_1}_{k-1})$ to $\hat{\mathbf{x}}^4(t^{s_1}_{k-1}|t^{s_2}_k)$ by the OOSM $z(t^{s_2}_k)$ — it fuses the latter into the former. Note that the sigma points of $\hat{\mathbf{x}}^4(t^{s_1}_{k-1}|t^{s_1}_{k-1})$ have been generated in (20).

According to the MMSE estimator [2], $\hat{\mathbf{x}}^4(t^{s_1}_{k-1}|t^{s_2}_k)$ and its error covariance $\mathbf{P}^4(t^{s_1}_{k-1}|t^{s_2}_k)$ are

$$\hat{\mathbf{x}}^4(t^{s_1}_{k-1}|t^{s_2}_k) = \hat{\mathbf{x}}^4(t^{s_1}_{k-1}|t^{s_1}_{k-1}) + \mathbf{P}_{xz} P^{-1}_{zz}[z(t^{s_2}_k) - \hat{z}(t^{s_2}_k)] \tag{42}$$

$$\mathbf{P}^4(t^{s_1}_{k-1}|t^{s_2}_k) = \mathbf{P}^4(t^{s_1}_{k-1}|t^{s_1}_{k-1}) - \mathbf{P}_{xz} P^{-1}_{zz} \mathbf{P}'_{xz} \tag{43}$$

The expected measurement $\hat{z}(t^{s_2}_k)$ is based on the retrodicted state $\hat{\mathbf{x}}^{5,m}(t^{e_2}_j|t^{s_1}_{k-1})$ as

$$\hat{z}(t^{s_2}_k) = \sum_{m=-4}^{4} w^m \hat{z}^m(t^{s_2}_k) \tag{44}$$

where

$$\begin{aligned}\hat{z}^m(t^{s_2}_k) &= h\left[\hat{\mathbf{x}}^{5,m}(t^{e_2}_j|t^{s_1}_{k-1})\right] \\ &= \tan^{-1}\left[\frac{x^m(t^{e_2}_j|t^{s_1}_{k-1}) - x^s(t^{s_2}_k)}{y^m(t^{e_2}_j|t^{s_1}_{k-1}) - y^s(t^{s_2}_k)}\right]\end{aligned} \tag{45}$$

The variance P_{zz} of the innovation and the covariance $\mathbf{P}_{xz}$ are computed by

$$P_{zz} = \sum_{m=-4}^{4} w^m [\tilde{z}^m(t^{s_2}_k)]^2 + R(t^{s_2}_k) \tag{46}$$

$$\mathbf{P}_{xz} = \sum_{m=-4}^{4} w^m \tilde{\mathbf{x}}^{4,m}(t^{s_1}_{k-1}|t^{s_1}_{k-1}) \tilde{z}^m(t^{s_2}_k) \tag{47}$$

$$\tilde{\mathbf{x}}^{4,m}(t^{s_1}_{k-1}|t^{s_1}_{k-1}) = \hat{\mathbf{x}}^{4,m}(t^{s_1}_{k-1}|t^{s_1}_{k-1}) - \hat{\mathbf{x}}^4(t^{s_1}_{k-1}|t^{s_1}_{k-1}) \tag{48}$$

$$\tilde{z}^m(t^{s_2}_k) = \hat{z}^m(t^{s_2}_k) - \hat{z}(t^{s_2}_k) \tag{49}$$

The OOSM-UGHF does not create new states, it only updates the states generated by the bearings from s_1 before.

IV. Simulation Results

Simulation results are preseued to demonstrate the new algorithm's performance. The conventional BOT approach is also evaluated using the same simulation data. Two sensor platform scenarios are used in the simulation tests:

- **Maneuvering (M)**: It has three legs linked by two $90^{\rm o}$ turns with turn rate $3^{\rm o}/{\rm s}$ shown in Fig. 2. The platform speed is 10m/s throughout the whole path. It moves to the east for 60s, spends 30s to make a $90^{\rm o}$ left turn, and moves to the north for 60s. It then makes a $90^{\rm o}$ right turn, and moves towards the east for 180s. The total duration is 360s.
- **Stationary (S)**: The platform stays at position (0m, 0m) for 360s.

An ESM sensor and an acoustic sensor are deployed on the platform to detect target bearings regularly. The two sensors are not synchronized. Their sampling intervals and initial detection times are different. The ESM sensor is initiated at time 0s with sampling interval 1s, whereas, the acoustic sensor is initiated at time 0.2s with sampling interval 2s. The measured bearing errors of the ESM and the acoustic sensors are zero-mean white Gaussian with standard deviations $\sigma_b = 1^{\rm o}$. Both sensors have no bearing detection during turns (total missed detection duration is 60s for the maneuvering platform scenarios).

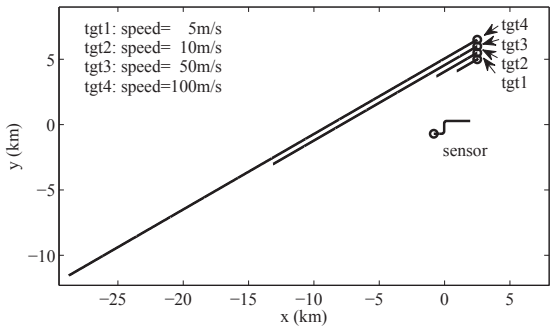

Fig. 2. Test scenarios. Initial locations of the targets and the maneuvering sensor platform are shown as "o". The stationary platform is not shown in the figure.

Four targets moving at constant speeds of 5m/s, 10m/s, 50m/s and 100m/s respectively are shown in Fig. 2. The state estimation starts 50s later after targets move from their initial positions, so the acoustic signal can be guaranteed to reach the sensor platform when estimation starts. This means that the targets are at their initial points at time –50s, and the sensor platform is at its initial point at time 0s. The estimation starts at time 0s.

The algorithms used in the simulation are:

- **OOSM-AE**: The acoustic-ESM fusion algorithm proposed in this paper. The OOSM-UGHF is applied to the bearings from the acoustic sensor, and the UKF is used to the bearings from the ESM. It works for both stationary and moving (maneuvering or nonmaneuvering) platform.
- **UKF-E**: A UKF to estimate state based on the ESM bearings only. The acoustic bearings are regarded as "expired" information and discarded. This algorithm is considered as a conventional BOT approach which works for maneuvering platform only.

The initial state estimate is[2]

$$\hat{\mathbf{x}}^4(t_0^{s_1}) = [\ \hat{r}_0 \sin b_0 \quad \hat{r}_0 \cos b_0 \quad 0 \quad 0\ ]' \tag{50}$$

where $\hat{r}_0$ is set to 10000m which is more than 4000m away from the ground truth ($r_0 = 4000{\rm m} \sim 6000{\rm m}$), and $b_0 = b(t_0^{s_1})$ is the ESM measured bearing at time $t_0^{s_1} = 0$s. The initial state error covariance is computed by [19]

$$\mathbf{P}^4(t_0^{s_1}) = \begin{bmatrix} P_{xx} & P_{xy} & 0 & 0 \\ P_{yx} & P_{yy} & 0 & 0 \\ 0 & 0 & 900 & 0 \\ 0 & 0 & 0 & 900 \end{bmatrix} \tag{51}$$

where

$$P_{xx} = (\hat{r}_0 \sigma_b \cos b_0)^2 + (\sigma_r \sin b_0)^2 \tag{52}$$
$$P_{yy} = (\hat{r}_0 \sigma_b \sin b_0)^2 + (\sigma_r \cos b_0)^2 \tag{53}$$
$$P_{xy} = P_{yx} = (\sigma_r^2 - \hat{r}_0^2 \sigma_b^2) \sin b_0 \cos b_0 \tag{54}$$

where $\sigma_r = \hat{r}_0/3$ is the initial range error standard deviation. The process noise PSD q in (7) is set to $0.01{\rm m}^2/{\rm s}^3$. The acoustic propagation speed $c^{\rm p}$ in the air is 344m/s. The scalar κ in (20)–(25) is set to 1.

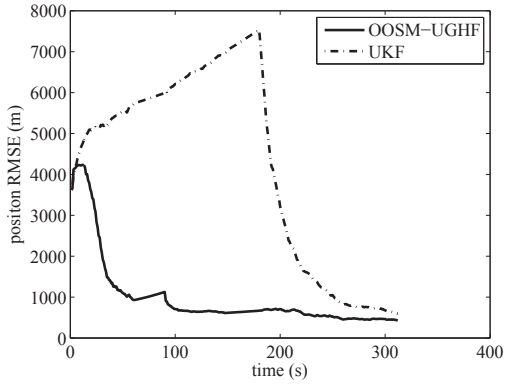

Fig. 3. Maneuvering platform: The estimated position RMSE versus time for the target with speed 5m/s.

The simulation results were obtained from 100 Monte Carlo runs. The estimated position root mean square errors (RMSE) versus time are displayed in Figs. 3–8, where Figs. 3–6 are for the maneuvering platform, and Figs. 7–8 are for the stationary platform. The overall and the last point position RMSEs for all the scenarios are given in Table I. The RMSEs of the UKF-E are not shown in this table for the stationary platform, for the targets are unobservable in this case. The

[2]We assume that the first bearing of a target is received from the EO/ESM sensor, as it is natural that the non-acoustic signal of a target reaches the sensor platform earlier than the acoustic signal.

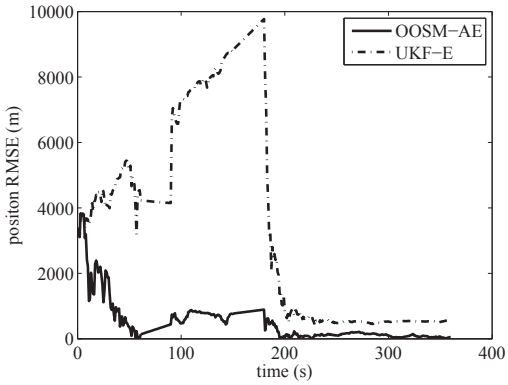

Fig. 4. Maneuvering platform: The estimated position RMSE versus time for the target with speed 10m/s.

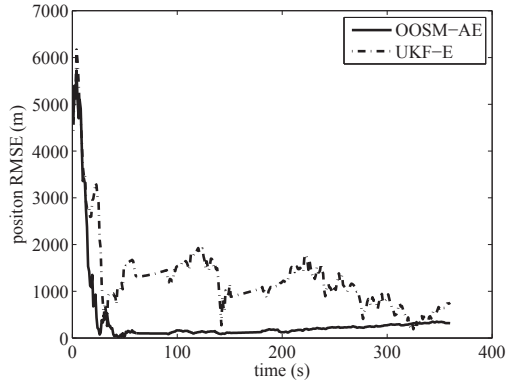

Fig. 5. Maneuvering platform: The estimated position RMSE versus time for the target with speed 50m/s.

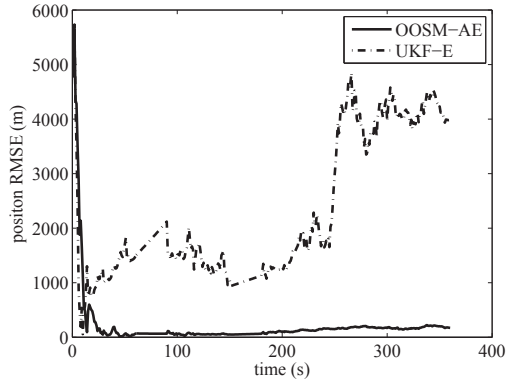

Fig. 6. Maneuvering platform: The estimated position RMSE versus time for the target with speed 100m/s.

overall position RMSE for a particular scenario is computed

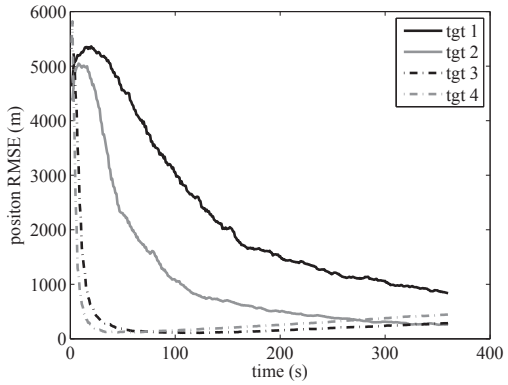

Fig. 7. Stationary platform: The OOSM-AE estimated position RMSE versus time for the targets with speeds of 5m/s (tgt 1), 10m/s (tgt 2), 50m/s (tgt 3) and 100m/s (tgt 4).

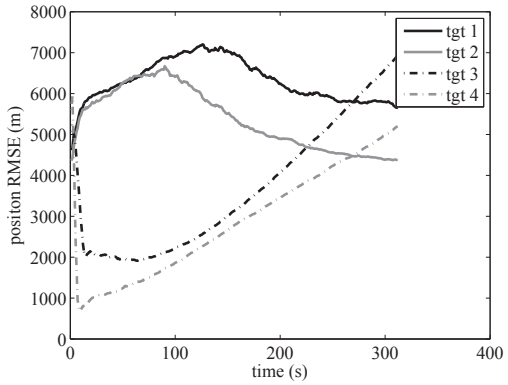

Fig. 8. Stationary platform: The UKF-E estimated position RMSE versus time for the four targets with speeds of 5m/s (tgt 1), 10m/s (tgt 2), 50m/s (tgt 3) and 100m/s (tgt 4).

TABLE I. POSITION RMSES FOR ALL THE SCENARIOS

Platform	Target speed (m/s)	Overall RMSE OOSM-AE (m)	Overall RMSE UKF-E (m)	Overall RMSE Impro-vement (%)	Last point RMSE OOSM-AE (m)	Last point RMSE UKF-E (m)
M	5	1132.3	4154.1	72.7	114.9	402.8
	10	831.6	4795.7	85.5	46.7	558.9
	50	806.9	1530.8	47.3	315.5	755.0
	100	605.2	2624.7	79.9	171.8	3975.4
S	5	2724.2	-	-	836.2	-
	10	1708.2	-	-	261.3	-
	50	755.7	-	-	286.7	-
	100	624.2	-	-	445.0	-

by

$$\mathrm{pos}^{\mathrm{RMSE}} = \sqrt{\frac{1}{NK}\sum_{i=1}^{N}\sum_{k=1}^{K}[\mathrm{pos}_i^{\mathrm{err}}(t_k^{s_1})]^2} \qquad (55)$$

where i is the run index, $N = 100$ is the number of runs, $K = 360$ is the number of time cycles in the scenario, and

$$\mathrm{pos}^{\mathrm{err}}(t_k^{s_1}) = \sqrt{[\hat{x}(t_k^{s_1}) - x(t_k^{s_1})]^2 + [\hat{y}(t_k^{s_1}) - y(t_k^{s_1})]^2} \quad (56)$$

where $\hat{x}(t_k^{s_1})$ and $\hat{y}(t_k^{s_1})$ are the estimated target positions, and $x(t_k^{s_1})$ and $y(t_k^{s_1})$ are the true target positions.

It can be seen that the OOSM-AE clearly outperforms the UKF-E for the maneuvering platform scenarios. The overall accuracy improvement in terms of position RMSE is from 47% to 86%, a significant improvement. For the slow moving targets (shown in Figs. 3–4), the UKF-E takes a longer time to converge. The UKF-E position RMSEs start to decrease at time 180s (after the second turn), whereas the RMSE reduction of the OOSM-AE occurs around time 25s, which is much earlier than for the UKF-E. For the fast moving targets (shown in Figs. 5–6), both algorithms converge fast at the beginning, but the UKF-E has larger errors after a while.

For the stationary platform (Figs. 7–8), the OOSM-AE provides reliable estimation, whereas the UKF-E diverges since BOT from a single ESM sensor is not observable.

We also observe that the OOSM-AE has better performance for the fast moving targets than the slow moving targets in both maneuvering and stationary platform scenarios. The reason for this is that the slow moving targets have lower bearing change rate. The information provided by these slow changed bearings is limited when they are "buried in the noise", and this results in marginal observability and slow convergence at the beginning. This effect is more serious for the stationary platform as its bearing change rate is even smaller than for the maneuvering platform.

V. Conclusions

This paper presented a new passive BOT approach through fusion of an ESM/EO and an acoustic sensor deployed on the same sensor platform. The OOSM-AE algorithm has been developed to estimate the target trajectory by utilizing the acoustic propagation delay which contains target range information. This approach avoids the requirement for platform maneuvers of the conventional BOT. Simulation results showed that the OOSM-AE can estimate the target trajectory effectively for the stationary platform, and provides significant accuracy improvement (47%–85%) over the conventional BOT for the maneuvering platform. This new approach has significant potential to enhance passive BOT capability significantly.

References

[1] Aidala, V. J.,"Kalman filter behavior in bearings-only tracking applications," *IEEE Transactions on Aerospace and Electronic Systems*, 15, 1 (Jan. 1979), 29-39.

[2] Bar-Shalom, Y., Li, X. R. and Kirubarajan, T., *Estimation with Applications to Tracking and Navigation: Theory, Algorithms and Software*, New York: Wiley, 2001.

[3] Bar-Shalom, Y., "Update with out-of-sequence measurements in tracking: Exact Solution," *IEEE Transactions on Aerospace and Electronic Systems*, 38, 3 (Jul. 2002), 769-778.

[4] Bar-Shalom, Y., Chen, H. M., and Mallick, M., "One-Step Solution for the Multistep Out-of-Sequence Measurement Problem in Tracking," *IEEE Transactions on Aerospace and Electronic Systems*, 40, 1 (Jan. 2004), 27-37

[5] Bar-Shalom, Y., Willett, P. K. and Tian, X., *Tracking and Data Fusion: A Handbook of Algorithms*, YBS Publishing, 2011.

[6] Le Cadre, J. P. and Jauffret, C., "Discrete-time observability and estimability analysis for bearings-only target motion analysis," *IEEE Transactions on Aerospace and Electronic Systems*, 33, 1 (Jan. 1997), 178-201.

[7] Clavard, J., Pillon, D., Pignol, A-C. and Jauffret, C., "Target motion analysis of a source in a constant turn from a nonmaneuvering observer," *IEEE Transactions on Aerospace and Electronic Systems*, 49, 3 (Jul. 2013), 1760-1780.

[8] Deb, S., Yeddanapudi, M., Pattipati, K. R. and Bar-Shalom, Y., "A generalized S-D assignment algorithm for multisensor-multitarget state estimation," *IEEE Transactions on Aerospace and Electronic Systems*, 33, 2 (Apr. 1997), 523-538.

[9] Hilton, R. D., Martin, D. A., and Blair, W. D., "Tracking with time-delayed data in multisensor systems," NSWCDD/TR-93/351, Dahlgren, VA, Aug. 1993.

[10] Jauffret C. and Bar-Shalom, Y., "Track Formation with Bearing and Frequency Measurements in Clutter," *IEEE Transactions on Aerospace Electronic Systems*, 26, 6 (Nov. 1990), 999-1009.

[11] Jauffret, C. and Pillon, D., "Observability in passive target motion analysis," *IEEE Transactions on Aerospace and Electronic Systems*, 32, 4 (Oct.1996), 1290-1300.

[12] Jauffret, C., Pillon, D., and Pignol, A-C., "Bearings-only maneuvering target motion analysis from a nonmaneuvering platform," *IEEE Transactions on Aerospace and Electronic Systems*, 46, 4 (Oct. 2010), 1934-1948.

[13] Julier, S. J., and Uhlmann, J. K., "A new extension of the Kalman filter to nonlinear systems," *Proceedings of AeroSense: The 11th International Symposium on Aerospace/Defence Sensing, Simulation and Controls*, Apr. 1997.

[14] Kirubarajan, T., Bar-Shalom, Y., and Lerro, D., "Bearings-only tracking of maneuvering targets using a batch-recursive estimator," *IEEE Transactions on Aerospace and Electronic Systems*, 37, 3 (Jul. 2001), 770-780.

[15] Lindgren, A. G. and Gong, K. F., "Position and velocity estimation via bearing observations," *IEEE Transactions on Aerospace and Electronic Systems*, 14, 4 (Jul. 1978) 564-577.

[16] Nardone, S. C. and Aidala, V. J., "Observability criteria for bearings-only target motion analysis," *IEEE Transactions on Aerospace and Electronic Systems*, 17, 2 (Mar. 1981), 162-166.

[17] Passerieux, J. M., Pillon, D., Blanc-Benon, P. and Jauffret, C., "Target Motion Analysis with Bearing and Frequencies Measurements," *Proceedings of the 22nd Asilomar Conference*, Pacific Grove, CA, USA, Nov. 1988.

[18] Pattipati, K. R., Deb, S., and Bar-Shalom, Y., "A new relaxation algorithm and passive sensor data association," *IEEE Transactions on Automatic Control*, 37, 2 (Feb. 1992), 198-213.

[19] Ristic, B., Arulampalam, S. and Gordon N., *Beyond the Kalman Filter: Particle Filters for Tracking Applications*, Boston London: Artech House, 2004.

[20] Yang, R., Bar-Shalom, Y. and Ng, G. W., "Tracking/fusion and deghosting with Doppler frequency from two passive acoustic sensor," *Proc. 16th International Conference on Information Fusion*, Istanbul, Turkey, Jul. 2013.

[21] Yang, R., Bar-Shalom, Y., Huang, J. H. and Ng, G. W., "Interacting multiple model unscented Gauss-Helmert filter for bearings-only tracking with state-dependent propagation delay," *Proc. 17th International Conference on Information Fusion*, Salamanca, Spain, Jul. 2014.

[22] Yang, R., Bar-Shalom, Y., Huang, J. H. and Ng, G. W., "Unscented Gauss-Helmert filter for bearings-only tracking with state-dependent propagation delay," to appear in *IEEE Transactions on Aerospace and Electronic Systems*, 2015.